NSRRC-Journal (2014)

Soft Matter

PAPER

View Article Online
View Journal | View Issue

Published on 23 December 2013. Downloaded by Synchrotron Radiation Library on 07/04/2014 02:47:51.

Cite this: *Soft Matter*, 2014, **10**, 2313

Formation of divalent ion mediated anionic disc bicelle–DNA complexes†

Po-Wei Yang,[a] Tsang-Lang Lin,*[a] Yuan Hu[a] and U-Ser Jeng[b]

Disc-shaped bicelles are formed by mixing long-chain lipids with short-chain lipids at suitable molar ratios and they have a relatively uniform size, typically around a few tens of nanometers in diameter. Different from the typically formulated cationic or anionic liposome–DNA complexes, which are used as nonviral vectors for improving the transfection efficiency of gene therapy, a novel way of packing the DNA can be developed by using the much smaller disc-like bicelles. We demonstrate that anionic lipid bicelle-ion–DNA (AB–DNA) complexes can be formed with the help of divalent ions. Multi-stacked AB–DNA complexes can be formed with diameters of around 50–100 nm and lengths of around 50–150 nm as revealed by TEM. Using the anionic lipid–DNA complexes has the advantage of lower cytotoxicity than using cationic lipids. The interaction of DNA with anionic bicelles was investigated by SAXS. It was found that the anionic bicelle could not form stable complexes with DNA at low calcium ion concentrations, such as 1 mM. The AB–DNA complexes can be formed in the investigated range of 10 mM to 100 mM calcium ion concentrations. However, for an equal anionic lipid charge and DNA charge system, an ion-membrane phase (multilamellar vesicles) would gradually appear as the calcium ion concentration is increased above a critical concentration. It indicates that DNA could be packed closer at above the critical divalent ion concentration. If more DNA is added to such a two-phase coexistence system (originally with the total anionic lipid charge equal to that of DNA), the ion-membrane phase could be transformed into the AB–DNA complexes. As a result, more DNA can be packed in the form of AB–DNA complexes at above the critical calcium ion concentration.

Received 3rd November 2013
Accepted 20th December 2013

DOI: 10.1039/c3sm52775a

www.rsc.org/softmatter

Introduction

There have been great efforts in recent years to develop gene delivery systems with high transfection efficiency by using both viral and nonviral vectors.[1–5] Viral vectors have higher transfection efficiency but there are concerns of safety and negative side effects in using them.[4,6] As a result, nonviral vectors have received great attention in recent years, such as using cationic lipids and block copolymers for forming complexes with negatively charged DNA.[2,7–12] Through charge interactions, DNA molecules can be stably encapsulated in cationic liposomes. Such cationic lipid–DNA (CL–DNA) complexes are immunogenic and have a high DNA packing capacity.[13–15] Although the synthetic cationic lipids could form stable complexes with DNA easily, there are concerns about their cytotoxicity.[16] It is desirable to develop alternative ways of complexing DNA without involving synthetic cationic lipids. It was found that anionic lipids can also form complexes with DNA, the anionic liposome–DNA complexes (AL–DNA), with the help of multivalent cations.[17–19] In order to form the anionic lipid–DNA complex, it is necessary to add multivalent cations that serve as a glue between the negatively charged DNA and the anionic lipids.[18] The phase behavior and structure of CL–DNA complexes are mainly determined by the membrane charge density and the charge lipid to DNA ratio as well.[9,18,20,21] For CL–DNA complexes, upon increasing the membrane positive charge density, the complex can vary from excess DNA to excess liposome.[21–23] As for the AL–DNA complexes, its phase behavior differs greatly from the CL–DNA complexes. Anionic lipid, such as 1,2-dimyristoyl-*sn-glycero*-3-phosphoglycerol (DMPG), is known to have quite different phase behavior as compared with zwitterionic lipids.[24,25] The multivalent ion mediated lipid membrane-ion–DNA lamellar structure of the AL–DNA can only exist at low membrane charge densities (50% or less) and in a suitable divalent ion concentration range.[18] At high membrane charge densities or low divalent ion concentrations, the lipid membrane-ion–DNA lamellar structure could be transformed into an ion-membrane structure by expelling out the DNA.[18] At high divalent ion concentrations, the lipid membrane-ion–DNA lamellar structure is no longer stable and can be transformed into the inverted columnar hexagonal phase.[18] Although the

[a]*Department of Engineering and System Science, National Tsing Hua University, Hsinchu, Taiwan, Republic of China. E-mail: tllin@mx.nthu.edu.tw; Fax: +886-3-5728445; Tel: +886-3-5742671*

[b]*National Synchrotron Radiation Research Center (NSRRC), Hsinchu, Taiwan, Republic of China*

† Electronic supplementary information (ESI) available. See DOI: 10.1039/c3sm52775a

This journal is © The Royal Society of Chemistry 2014

Published on 23 December 2013. Downloaded by Synchrotron Radiation Library on 07/04/2014 02:47:51.

phase behaviors of such multivalent ion mediated anionic lipid–DNA aggregates are more complex and sensitive to membrane charge density and the divalent ion concentration, it is still desirable to use the AL–DNA complexes due to their low cytotoxicity.

Alternatively, in this study, a more robust and smaller size anionic lipid–DNA complex system is developed by using anionic disc bicelles to form the anionic bicelle-ion–DNA complexes (AB–DNA). Disc-like bicelles have been widely used as model membrane systems for investigating the protein–membrane interactions.[26] Bicelles have a typical diameter of around 25 nm and a thickness of a lipid bilayer and they can be spontaneously formed in aqueous solutions by mixing long-chain lipids with short-chain lipids at suitable ratios.[27–30] The long-chain lipids form a planar bilayer core and the short-chain lipids form a protecting ring around the rim of the disc bilayer core. The structure of the disc bicelle is stable at temperatures below the melting temperature of long-chain lipid constituting the planar region. Bicelles can be doped with anionic lipids to become anionic bicelles. Due to their relatively small size, it is possible to formulate small size anionic lipid-ion–DNA complexes mediated by the multivalent ions. However, it is not clear as to how the divalent ion concentration affects the formation of such AB–DNA complexes. In this study, the effect of the divalent ion concentration on the structure and the phase behavior of such AB–DNA complexes were investigated by small-angle X-ray scattering (SAXS) and transmission electron microscopy (TEM). It is aimed at understanding the structural characteristics and the stability of such AB–DNA complexes in order to develop alternative ways of packing DNA for biomedical and other related applications.

Experimental section

Materials and sample preparation

The long chain zwitterionic lipid 1,2-dihexadecanoyl-*sn-glycero*-3-phosphocholine (DPPC), short chain zwitterionic lipid 1,2-diheptanoyl-*sn-glycero*-3-phosphocholine (diC7PC), and anionic lipid 1,2-dipalmitoyl-*sn-glycero*-3-phospho-(1′-*rac*-glycerol) (sodium salt) (DPPG) were purchased from Avanti Co. Linear DNA (type XIV) from herring testes, sodium salt was purchased from Sigma. The molecular weight of the DNA determined by gel electrophoresis was between 400 and 1000 base pairs (a base pair has a molecular weight of 649 g mol^{-1}) with an averaged value of 700 base pairs.[31] In this study, the ratio of the short-chain lipids to the total long chain lipids (DPPC plus DPPG) is kept at 3 to 1 in order to form the disc-like bicelles in aqueous solutions at a total lipid concentration of 13.33 mM. The long-chain lipids consist of 15% DPPG and 85% DPPC. DPPC and diC7PC were dissolved in chloroform, while DPPG was dissolved in chloroform–methanol at a 9/1 (vol/vol) mixing ratio. The appropriate amounts of the prepared solutions were mixed at designated ratios. The mixtures were evaporated and then kept in a vacuum oven for at least 8 hours to remove all the traces of organic solvents completely. Subsequently, the dry residues were rehydrated by adding 1.07 μM DNA aqueous solution (containing calcium chloride at designated concentrations) for most of the samples and treated by bath sonication at a temperature of about 30 °C for 5 minutes in order to homogenize the bicelle–DNA suspensions in H_2O. The charge ratio of the 1.07 μM DNA to the 1.5 mM anionic DPPG lipid is equal to 1.

Small-angle scattering (SAS) and transmission electron microscopy (TEM)

SAXS measurements were carried out at the SAXS beamline 23A at the National Synchrotron Research Center (NSRRC), Hsinchu, Taiwan.[32] The photon energy and the sample-to-detector distance were set at 14 keV ($\Delta E/E$ = 1/7000) and 2700 mm, respectively, in order to cover a scattering vector, $Q = (4\pi/\lambda)\sin(\theta/2)$, from 0.008 to 0.35 $Å^{-1}$. Here, λ is the X-ray wavelength and θ is the scattering angle. The liquid samples were sealed in a sample cell with 5 mm thickness and a Kapton-walled window. The samples were kept at 25 °C during the measurements. Scattered X-rays were collected by a MarCCD detector. The collected 2D data were circularly averaged to obtain the 1D scattering intensity *versus* scattering vector distribution. The measured scattering intensity was corrected for detector sensitivity, background, and normalized to obtain the absolute scattering cross sections. For preparing the TEM samples, the samples were first diluted, then dripped onto a copper grid with a supported membrane. Any extra solution was sopped out by filter paper. In order to enhance the sample contrast, negative-staining was applied to the samples by adding uranyl acetate (1 wt%) for 30 seconds.[30,33] TEM images were taken at an e-beam energy of 100 kV using a JEOL JEM-1230 of Chang Gung University, Taiwan.

Results and discussions

The multivalent cation plays critical roles in the formulation of the AB–DNA or AL–DNA complexes. Fig. 1 shows the measured small-angle X-ray scattering profiles of the mixed DPPC/DPPG/diC7PC samples (at 8.5, 1.5, 3.33 mM, respectively), without and with 1.07 μM DNA at various calcium ion concentrations.

The scattering profile of the pure anionic bicelles is similar to that of typical DPPC/diC7PC bicelles except the appearance of a broad correlation peak in the low-Q region (around $Q = 0.01$ $Å^{-1}$) due to the charge interaction between the anionic bicelles.[30] Upon the addition of DNA to the pure anionic bicelles, the SAXS profile of the anionic bicelle–DNA sample still resembles the scattering profile of the pure anionic bicelles, which indicates that the anionic bicelles do not form complexes with DNA in the absence of multivalent cations. Due to the charge repulsion, the negatively charged DNA molecules will not associate with the anionic bicelles. Upon the addition of 10 mM Ca^{2+}, well-defined diffraction peaks ($Q_{I,1} = 0.079$ $Å^{-1}$, $Q_{I,2} = 0.158$ $Å^{-1}$, *etc.*) emerge in the scattering profile which indicates the existence of a lamellar structure of AB–DNA complexes mediated by divalent cations.

The anionic bicelles, though smaller than the length scale of the DNA, can still bind DNA arrays to form stable ordered multi stacks with the help of divalent cations. The corresponding

 This journal is © The Royal Society of Chemistry 2014

Published on 23 December 2013. Downloaded by Synchrotron Radiation Library on 07/04/2014 02:47:51.

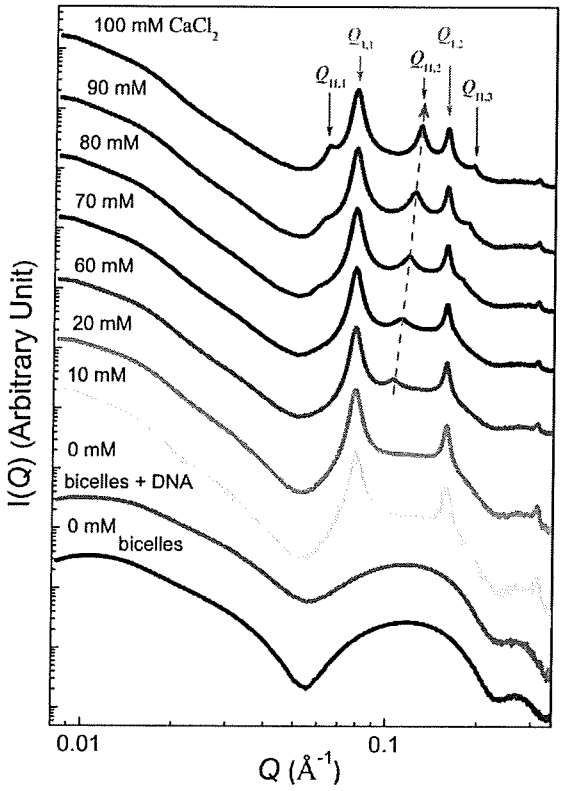

Fig. 1 The measured small-angle X-ray scattering profiles of the mixed DPPC/DPPG/diC7PC samples (at 8.5, 1.5, 3.33 mM, respectively), without and with 1.07 μM DNA at various calcium ion concentrations (as indicated on each curve) at 25 °C. The scattering curves are shifted for clarity. All the cases contain 1.07 μM DNA except for the pure mixed lipid (anionic bicelle) system.

d-spacing, $2\pi/Q_{peak} = 79.5$ Å, of the AB–DNA lamellar structure is in accordance with the d-spacing of the AL–DNA complexes.[18] This d-spacing corresponds to the ordered bilayer-ion–DNA–ion-bilayer structural model with a lipid bilayer thickness of around 53 Å, DNA diameter of 20 Å, and two layers of calcium ions of 4 Å each.[18] Unlike the cationic bicelle–DNA (CB–DNA) complexes (see Fig. S1 in the ESI†), there is no clear in-plane correlation peak from the DNA array encapsulated between disc bicelles for the AB–DNA complexes. The absence of the DNA–DNA correlation peak is similar to the AL–DNA complexes mediated by divalent ions.[18] The DNA molecules are not as rigidly held between the lipid bilayers in the AB–DNA system as compared with the AL–DNA system since the DNA molecules in the AB–DNA system are bound to the lipid bilayer through the more dynamic calcium ions. Upon further increase of the calcium ion concentration to 100 mM, both the positions of these diffraction peaks and their full width at half maximum (FWHM) remain unchanged. The d-spacing of the AB–DNA complexes does not change with the increase of calcium ion concentration. Even with the addition of more calcium ions, there is still only one array/layer of DNA molecules encapsulated between the lipid bilayers as mediated by the divalent ions. This bilayer-ion–DNA lamellar structure is quite stable against the changes in DNA or calcium ion concentrations due to the strong charge interactions between the DNA and the anionic lipid mediated by the divalent ions. However, at calcium ion concentrations above 60 mM, another set of lamellar diffraction peaks, $Q_{II,1}$, $Q_{II,2}$ and $Q_{II,3}$ gradually appear, as indicated in Fig. 1. The positions of these additional diffraction peaks shift to higher Q positions as the calcium ion concentration is increased. The d-spacing of this lamellar phase decreases from ~12 nm to ~10 nm as the calcium ion concentration increases from 60 to 100 mM. The variation of the d-spacing of these two lamellar phases as a function of the calcium ion concentration is shown in Fig. 2.

In order to understand the origin of this lamellar phase, the DPPG doped bicelles in the presence of 100 mM $CaCl_2$ but without DNA was also measured by SAXS for comparison with the case containing 1.07 μM DNA. As shown in Fig. 3, for the mixed DPPC/DPPG/diC7PC sample (at 8.5, 1.5, 3.33 mM, respectively), at 100 mM $CaCl_2$ but without 1.07 μM DNA, there is only one set of lamellar diffraction peaks, at $Q_{II,1} = 0.064$ Å^{-1} and $Q_{II,2} = 0.127$ Å^{-1}, which matches exactly the second set of lamellar diffraction peaks of the same sample system but with 1.07 μM DNA. The second lamellar phase in the DPPC/DPPG/diC7PC/DNA system appearing at higher calcium ion concentrations can be identified to be the ion-membrane complexes. The coexistence of these two phases at higher calcium ion concentrations indicates that calcium ions play critical roles in both the DNA–ion-membrane complexes and also in the ion-membrane complexes.

The calcium ion is one of the most common and important ions in living organisms and it involves in regulating the functions and cellular associated processes.[34,35] There were many studies on the effect of cations on zwitterionic DPPC

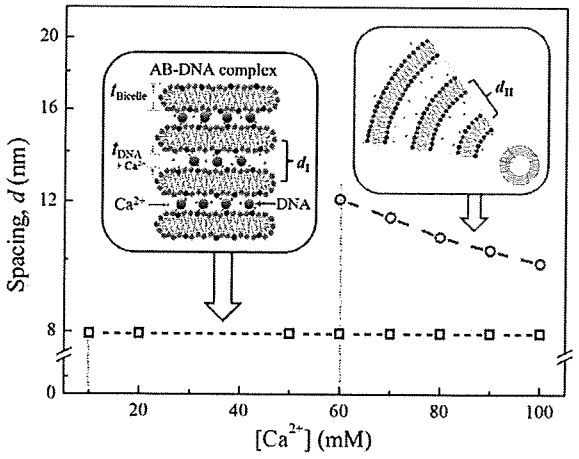

Fig. 2 The dependence of the d-spacing of the lamellar structures of AB–DNA and ion-membrane phases is shown as a function of the calcium ion concentration for the mixed DPPC/DPPG/diC7PC sample system (at 8.5, 1.5, 3.33 mM, respectively). The concentration of the DNA, 700 base pair on average, is 1.07 μM. Schematic pictures of these two phases are inserted. The side view of the self-assembled AB–DNA complex is shown schematically, where the semi flexible DNA of 700 or 2000 bp is presented as a green rod (a green dot for side view). The calcium ions are represented as red dots. The uncertainty of the values of d-spacing is less than 0.1%.

Published on 23 December 2013. Downloaded by Synchrotron Radiation Library on 07/04/2014 02:47:51.

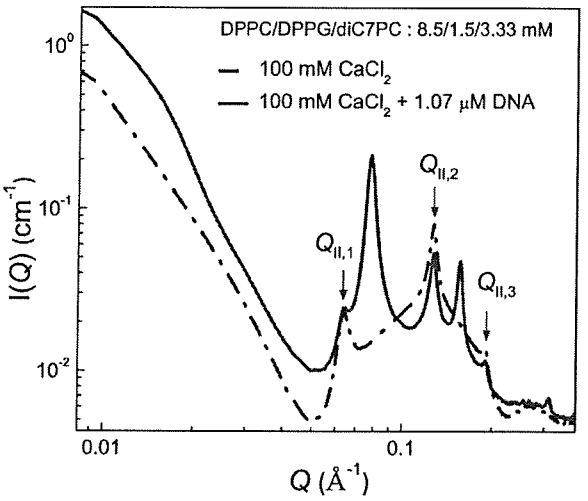

Fig. 3 The measured SAXS profiles of the mixed DPPC/DPPG/diC7PC samples (at 8.5, 1.5, 3.33 mM, respectively), with and without 1.07 μM DNA at 100 mM calcium ion concentration. For the mixed DPPC/DPPG/diC7PC sample, at 100 mM $CaCl_2$ without 1.07 μM DNA, there is only one set of lamellar diffraction peaks, at $Q_{II,1} = 0.064$ Å^{-1} and $Q_{II,2} = 0.127$ Å^{-1}, which matches exactly the second set of lamellar diffraction peaks of the same sample system but with 1.07 μM DNA. The second lamellar phase in the DPPC/DPPG/diC7PC/DNA system appearing at higher calcium ion concentrations can be identified to be the ion-membrane complexes.

model membranes by SAS,[36,37] and molecular dynamic (MD) simulations.[38–40] The presence of calcium ions could cause a decrease in the surface area per lipid head group,[37,41,42] an increase in membrane thickness,[37,41] and the increase of the gel to liquid phase transition temperature, T_m.[43] The effect of multivalent cations on the membranes containing anionic lipids differs greatly from their effects on zwitterionic bilayers since the cations can interact strongly with the negatively charged phospholipids through electrostatic forces.[44,45] MD simulations showed that calcium ions have high binding affinity to the anionic head group that would enhance the molecular packing and the ordering of bilayer.[45–47] As for anionic bicelles, without the regulation of calcium ions, the anionic bicelles containing 15% DPPG are well dispersed in aqueous solutions and the SAXS profile only exhibits the typical bicelle form factor with a broad correlation peak located around $Q = 0.01$ Å^{-1} that originates from the charge repulsion interaction between anionic bicelles (as shown in Fig. 1). In the presence of higher calcium ion concentrations, the charge repulsion between negatively charged bicelles is screened and the calcium ions could also induce bicelle aggregation to form a multi-bilayer structure (condensed ion-membrane complexes) (as shown in Fig. 3). The d-spacing of the ion-membrane complexes (the second set of the lamellar diffraction peaks in Fig. 1), as calculated from $d = 2\pi/Q_{II,1}$, decreases with increasing divalent ion concentrations. The binding force in ion-membrane complexes becomes stronger as the calcium ion concentration increases and the water gap between the membrane bilayers is reduced accordingly as the calcium ion concentration increases.

The DNA concentration is also an important factor in formulating the AB–DNA complexes. For 1.07 μM DNA, the charge ratio of the DNA to the 1.5 mM anionic DPPG lipid is equal to 1. Fig. 4 shows the measured SAXS profiles of the DPPC/DPPG/diC7PC samples (at 8.5, 1.5, 3.33 mM, respectively), at 100 mM calcium ion concentration, mixed with different amounts of DNA. As shown in Fig. 4, the lamellar diffraction peaks of the ion-membrane complexes, for example, the second diffraction peak at $Q_{II,2} = 0.157$ Å^{-1}, gradually disappears when the DNA concentration is increased from 1.07 μM to 4.28 μM. This indicates that the ion-membrane complexes are gradually turned into the DNA–ion-membrane complexes as more DNA is added. When there are more DNA molecules, it needs more lipid bilayers to encapsulate the DNA molecules. While the component of ion-membrane complexes decreases with increasing DNA concentrations, the DNA–ion-membrane component increases as evidenced from the increase of the diffraction peak intensity of the DNA–ion-membrane complexes. The formation of the DNA–ion-membrane complexes is obviously more favourable than the formation of ion-membrane complexes whenever there are DNA molecules available. The ion-membrane complexes would not be formed unless there is a surplus of free anionic bilayers which form at higher calcium ion concentrations. At higher calcium ion concentrations, fewer amounts of anionic bilayers are required to encapsulate the DNA and some excess anionic bilayers are released from the DNA–ion-membrane complexes to the ion-membrane complexes.

As shown in Fig. 4, the ion-membrane phase almost disappears as the DNA concentration is increased to 2.14 μM, and it disappears completely when the DNA concentration is increased to 4.28 μM. This implies that there will be no excess lipids for a DNA concentration slightly above 2.14 μM. At this no

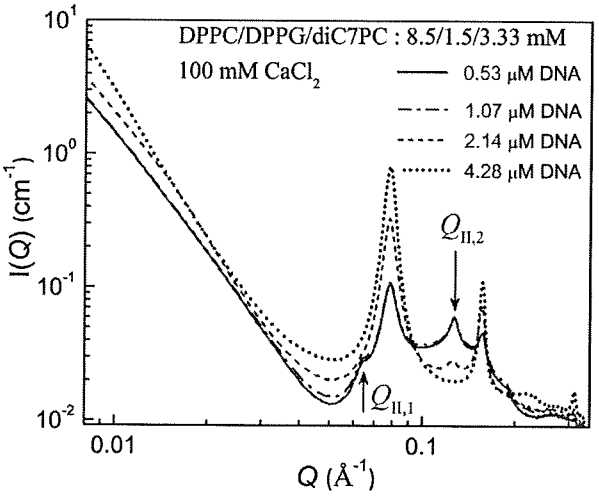

Fig. 4 The measured SAXS profiles of the mixed DPPC/DPPG/diC7PC samples (at 8.5, 1.5, 3.33 mM, respectively), with different amounts of DNA at 100 mM calcium ion concentration. The lamellar diffraction peaks of the ion-membrane complexes, for example, the second diffraction peak at $Q_{II,2} = 0.157$ Å^{-1}, gradually disappear when the DNA concentration is increased from 1.07 μM to 4.28 μM. The charge ratio of the 1.07 μM DNA to the 1.5 mM anionic DPPG lipid is equal to 1.

This journal is © The Royal Society of Chemistry 2014

Published on 23 December 2013. Downloaded by Synchrotron Radiation Library on 07/04/2014 02:47:51.

excess lipid point, the ratio of the DNA charge to the anionic lipid charge will be slightly above 2. At 1.07 μM DNA and 100 mM $CaCl_2$, the amounts of the excess lipids (forming the ion-membrane complexes in the presence of DNA) can be roughly estimated from the diffraction peak heights of the $Q_{II,2}$ in Fig. 3 for the cases with and without DNA. The excess lipids are estimated to be about 60% (assumed to be proportional to the peak height). This will imply that roughly 40% of the lipids are used to encapsulate the 1.07 μM DNA at 100 mM $CaCl_2$.

Multivalent ions play an important role in the charge lipid systems as well as polyelectrolytes, such as DNA. Charge interaction is one of the key forces in controlling the self-assembly of nanostructural materials. The presence of poly-cations with a valence of more than 2, such as spermidine (3^+) or spermine (4^+), could induce severe DNA condensation in aqueous solutions within a certain ion concentration range and redissolution occurs at higher ion concentrations.[48,49] As for divalent cations, they could not efficiently induce DNA condensation in bulk aqueous solutions. However, at the planar interfaces, DNA condensation could occur in the presence of divalent cations. For example, in the presence of divalent cations, DNA condensation to a cationic lipid monolayer or to a cationic diblock copolymer monolayer at the air–water interface was observed in reflectivity studies.[50–54] Furthermore, the degree of DNA condensation is governed by the concentration of divalent ions.[54,55] As a result, calcium ions could agglutinate the DNA array encapsulated between lipid bilayers at higher calcium ion concentrations as that happens in the cationic–DNA system.[56]

Other than the studies on the AB–DNA complex aggregation structure by SAXS, TEM was also employed to visualize the real-space images of the ion-mediated AB–DNA complex formation. As revealed by TEM, at low calcium ion concentrations, such as 1 mM, the calcium ion concentration is too low to induce the formation of the DNA–ion-membrane complexes and the anionic bicelles remain isolated, as shown in Fig. 5(A). As shown in Fig. 5(B) for the 10 mM calcium ion concentration case, the DNA–ion-membrane complexes can be clearly observed. The size of the disc bilayers forming the complexes is around 50 to 100 nm in diameter and they are less rigid (curved) as compared with the originally smaller isolated anionic bicelles with a diameter of about 25–35 nm. The length of the stacked AB–DNA complexes varies from 50 to 150 nm as observed in Fig. 5(B). The disc bicelles seem to fuse into a slightly larger bicelles when forming the DNA–ion-membrane complexes. Since the persistence length of DNA is around 50 nm, it is likely that the encapsulated DNA molecules could form a planar ordered array section of around 50 nm. Bicelles could fuse into a similar size to encapsulate the ordered DNA array section. Since the DNA average length is around 200 nm, probably both ends of the DNA are extending outside the disc bilayer. For the 100 mM calcium ion concentration case, two distinct phases, the AB–DNA complex and the ion-membrane complex in multilamellar vesicle form, respectively, can be easily identified in Fig. 5(C). These results are consistent with the deduction from SAXS analysis.

By summarizing the TEM and SAXS results, the *d*-spacing as a function of calcium ion concentration is given in Fig. 2 together with the schematic pictures of the DNA–ion-membrane

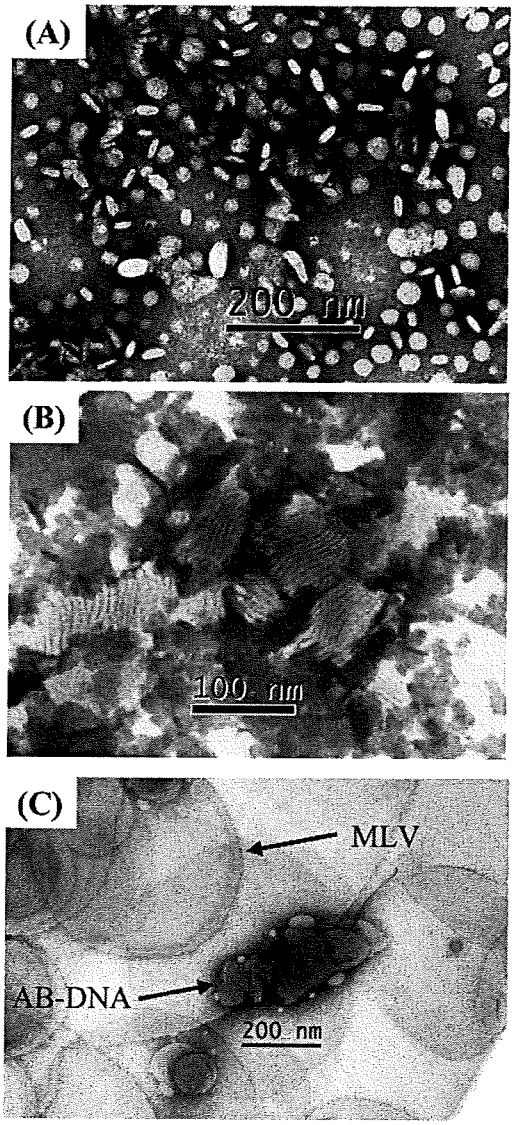

Fig. 5 TEM images of the mixed DPPC/DPPG/diC7PC samples (at 8.5, 1.5, 3.33 mM, respectively) with 1.07 μM DNA and calcium ion concentration of (A) 1 mM, (B) 10 mM, and (C) 100 mM. The AB–DNA complex and the multilamellar vesicle (MLV) are indicated in (C). As shown in (A), the disc-like bicelles remain isolated in the presence of DNA and 1 mM calcium ions. The formation of multi-stacked disc bilayer-ion–DNA complexes can be clearly observed in (B).

complex and the ion-membrane complex. The *d*-spacing of the AB–DNA lamellar structure, d_I, corresponding to the ordered disc bilayer-ion–DNA–ion-disc bilayer structure, remains unchanged when the concentration of calcium ions is increased from 10 to 100 mM. At above 60 mM calcium ion concentration, the ion-membrane phase begins to appear with a lamellar *d*-spacing, d_{II}, which gradually decreases with increasing calcium ion concentration. For the complexes formed by cationic lipid doped bicelles, the one-dimensionally stacked cationic bicelles–DNA (CB–DNA) complexes can be formed spontaneously without the help of calcium ions.[57] The *d*-spacing of the AB–DNA complexes is found to be slightly larger than the

Published on 23 December 2013. Downloaded by Synchrotron Radiation Library on 07/04/2014 02:47:51.

d-spacing of the CB–DNA complexes by about 4.7 Å (Fig. S1 in the ESI†). Obviously, the slightly larger *d*-spacing is caused by the existence of the calcium ion layers.

Conclusions

In summary, with sufficient amounts of calcium ions, the anionic bicelles could form complexes with the DNA in a DNA–ion-disc bilayer multi-stacked lamellar form. Using anionic lipids to formulate the lipid–DNA complexes could reduce the cytotoxicity in gene therapy. In addition to the lower cytotoxicity, the AB–DNA complexes have the advantage of smaller size than the conventional cationic lipid–DNA complexes in liposome or hexagonal packing forms or the anionic lipid-ion–DNA multilamellar vesicle form, which might help to improve the transfection efficiency. The *d*-spacing of such an AB–DNA complex does not change with increasing calcium ion concentrations. For an equal anionic lipid charge and DNA charge system, an ion-membrane phase (multilamellar vesicles) gradually appears as the calcium ion concentration is increased to above a critical concentration. The appearance of this ion-membrane phase is likely due to the compaction of the DNA array at above the divalent ion critical concentration and subsequently the release of the excess lipids to form the ion-membrane complexes. When more DNA molecules are added to such a two-phase coexistence system (originally with the total anionic lipid charges equal to that of DNA), the ion-membrane phase could be transformed into the AB–DNA complexes. Higher DNA packing density can be expected with anionic bicelles at calcium ion concentration above the critical calcium ion concentration.

Acknowledgements

We would like to thank the NSRRC for providing the synchrotron SAXS beamline and for the help in measurements, and the Chang Gung University for the TEM analysis. This research is supported by the National Science Council, project no. NSC 99-2113-M-007-014-MY3 and NSC 102-2113-M-007 -013 (T.-L. Lin). This research is also partly supported by the Frontier Research Center on Fundamental and Applied Sciences of Matters of National Tsing Hua University.

References

1 L. Naldini, U. Blomer, P. Gallay, D. Ory, R. Mulligan, F. H. Gage, I. M. Verma and D. Trono, *Science*, 1996, 272, 263–267.
2 K. Kataoka, A. Harada and Y. Nagasaki, *Adv. Drug Delivery Rev.*, 2001, **47**, 113–131.
3 D. Fischer, T. Bieber, Y. X. Li, H. P. Elsasser and T. Kissel, *Pharm. Res.*, 1999, **16**, 1273–1279.
4 M. A. Kay, J. C. Glorioso and L. Naldini, *Nat. Med.*, 2001, 7, 33–40.
5 M. A. Mintzer and E. E. Simanek, *Chem. Rev.*, 2009, **109**, 259–302.
6 C. E. Thomas, A. Ehrhardt and M. A. Kay, *Nat. Rev. Genet.*, 2003, **4**, 346–358.
7 A. V. Kabanov, E. V. Batrakova and V. Y. Alakhov, *J. Controlled Release*, 2002, **82**, 189–212.
8 T. G. Park, J. H. Jeong and S. W. Kim, *Adv. Drug Delivery Rev.*, 2006, **58**, 467–486.
9 J. O. Rädler, I. Koltover, T. Salditt and C. R. Safinya, *Science*, 1997, **275**, 810–814.
10 H. Farhood, N. Serbina and L. Huang, *Biochim. Biophys. Acta*, 1995, **1235**, 289–295.
11 P. Andreozzi, S. S. Funari, C. La Mesa, P. Mariani, M. G. Ortore, R. Sinibaldi and F. Spinozzi, *J. Phys. Chem. B*, 2010, **114**, 8056–8060.
12 L. Xu, L. Feng, R. Dong, J. Hao and S. Dong, *Biomacromolecules*, 2013, **14**, 2781–2789.
13 A. El-Aneed, An overview of current delivery systems in cancer gene therapy, *J. Controlled Release*, 2004, **94**, 1–14.
14 M. Morille, C. Passirani, A. Vonarbourg, A. Clavreul and J.-P. Benoit, *Biomaterials*, 2008, **29**, 3477–3496.
15 A. G. Schatzlein, *Anticancer Drugs*, 2001, **12**, 275–304.
16 X. Gao, K. S. Kim and D. X. Liu, *AAPS J.*, 2007, **9**, E92–E104.
17 S. D. Patil, D. G. Rhodes and D. J. Burgess, *AAPS J.*, 2004, **6**, 13–22.
18 H. J. Liang, D. Harries and G. C. L. Wong, *Proc. Natl. Acad. Sci. U. S. A.*, 2005, **102**, 11173–11178.
19 C. Montis, S. Milani, D. Berti and P. Baglioni, *J. Colloid Interface Sci.*, 2012, **373**, 57–68.
20 D. Pozzi, H. Amenitsch, C. Marchini and G. Caracciolo, *Appl. Phys. Lett.*, 2010, **96**, 183702–183703.
21 S. May, D. Harries and A. Ben-Shaul, *Biophys. J.*, 2000, **78**, 1681–1697.
22 I. Koltover, T. Salditt and C. R. Safinya, *Biophys. J.*, 1999, 77, 915–924.
23 D. Harries, S. May, W. M. Gelbart and A. Ben-Shaul, *Biophys. J.*, 1998, 75, 159–173.
24 F. Spinozzi, L. Paccamiccio, P. Mariani and L. Q. Amaral, *Langmuir*, 2010, **26**, 6484–6493.
25 F. Spinozzi, P. Mariani, L. Paccamiccio and L. Q. Amaral, *J. Phys.: Conf. Ser.*, 2010, **247**, 012019.
26 A. A. De Angelis, S. C. Howell, A. A. Nevzorov and S. J. Opella, *J. Am. Chem. Soc.*, 2006, **128**, 12256–12267.
27 T.-L. Lin, C.-C. Liu, M. F. Roberts and S.-H. Chen, *J. Phys. Chem.*, 1991, **95**, 6020–6027.
28 T. L. Lin, S. H. Chen, N. E. Gabriel and M. F. Roberts, *J. Am. Chem. Soc.*, 1986, **108**, 3499–3507.
29 J. Katsaras, T. A. Harroun, J. Pencer and M. P. Nieh, *Naturwissenschaften*, 2005, **92**, 355–366.
30 P. W. Yang, T. L. Lin, Y. Hu and U. S. Jeng, *Chin. J. Phys.*, 2012, **50**, 349–356.
31 M. Garcia-Diaz, O. Dominguez, L. A. Lopez-Fernandez, L. T. de Lera, M. L. Saniger, J. F. Ruiz, M. Parraga, M. J. Garcia-Ortiz, T. Kirchhoff, J. del Mazo, A. Bernad and L. Blanco, *J. Mol. Biol.*, 2000, **301**, 851–867.
32 U-S. Jeng, C. H. Su, C.-J. Su, K.-F. Liao, W.-T. Chuang, Y.-H. Lai, J.-W. Chang, Y.-J. Chen, Y.-S. Huang, M.-T. Lee, K. L. Yu, J. M. Lin, D. G. Liu, C. F. Chang, C. Y. Liu, C. H. Chang and K. S. Liang, *J. Appl. Crystallogr.*, 2010, **43**, 110–121.

 This journal is © The Royal Society of Chemistry 2014

Published on 23 December 2013. Downloaded by Synchrotron Radiation Library on 07/04/2014 02:47:51.

33 K. J. Glover, J. A. Whiles, G. Wu, N. J. Yu, R. Deems, J. O. Struppe, R. E. Stark, E. A. Komives and R. R. Vold, *Biophys. J.*, 2001, **81**, 2163–2171.
34 A. G. Lee, *Biochim. Biophys. Acta, Biomembr.*, 2004, **1666**, 62–87.
35 O. H. Petersen, M. Michalak and A. Verkhratsky, *Cell Calcium*, 2005, **38**, 161–169.
36 D. Uhrikova, J. Teixeira, A. Lengyel, L. Almasy and P. Balgavy, *Spectrosc. Int. J.*, 2007, **21**, 43–52.
37 D. Uhrikova, N. Kucerka, J. Teixeira, V. Gordeliy and P. Balgavy, *Chem. Phys. Lipids*, 2008, **155**, 80–89.
38 A. Cordomi, O. Edholm and J. J. Perez, *J. Phys. Chem. B*, 2008, **112**, 1397–1408.
39 R. D. Porasso and J. J. Lopez Cascales, *Colloids Surf., B*, 2009, **73**, 42–50.
40 S. A. Pandit, D. Bostick and M. L. Berkowitz, *Biophys. J.*, 2003, **84**, 3743–3750.
41 G. Pabst, A. Hodzic, J. Strancar, S. Danner, M. Rappolt and P. Laggner, *Biophys. J.*, 2007, **93**, 2688–2696.
42 R. A. Bockmann and H. Grubmuller, *Angew. Chem., Int. Ed.*, 2004, **43**, 1021–1024.
43 M. G. Ganesan, D. L. Schwinke and N. Weiner, *Biochim. Biophys. Acta, Biomembr.*, 1982, **686**, 245–248.
44 E. R. Lamberson, L. R. Cambrea and J. S. Hovis, *J. Phys. Chem. B*, 2007, **111**, 13664–13667.
45 P. T. Vernier, M. J. Ziegler and R. Dimova, *Langmuir*, 2009, **25**, 1020–1027.
46 U. R. Pedersen, C. Leidy, P. Westh and G. H. Peters, *Biochim. Biophys. Acta, Biomembr.*, 2006, **1758**, 573–582.
47 H. Y. Yang, Y. C. Xu, Z. B. Gao, Y. Y. Mao, Y. Du and H. L. Jiang, *J. Phys. Chem. B*, 2010, **114**, 16978–16988.
48 V. A. Bloomfield, *Curr. Opin. Struct. Biol.*, 1996, **6**, 334–341.
49 V. A. Bloomfield, *Biopolymers*, 1997, **44**, 269–282.
50 T. L. Lin, Y. Hu, J. C. Wu, C. P. Yang, U. Jeng and M. C. Shih, Slow Dynamics in Complex Systems, *AIP Conf. Proc.*, 2004, **708**, 328–329.
51 J. C. Wu, T. L. Lin, U. S. Jeng, H. Y. Lee and T. Gutberlet, *Phys. B*, 2006, **385–386**, 841–844.
52 J. C. Wu, T. L. Lin, U. S. Jeng and N. Torikai, *Phys. B*, 2006, **385–386**, 838–840.
53 T. L. Lin, J. C. Wu, U. S. Jeng and H. Y. Lee, *J. Appl. Crystallogr.*, 2007, **40**, S680–S683.
54 P. W. Yang, T. L. Lin, I. T. Liu, Y. Hu and M. James, *Soft Matter*, 2012, **8**, 7161–7168.
55 T. L. Lin, J. C. Wu, Y. Hu, U.-S. Jeng and H. Y. Lee, *Chin. J. Phys.*, 2012, **50**, 332–343.
56 I. Koltover, K. Wagner and C. R. Safinya, *Proc. Natl. Acad. Sci. U. S. A.*, 2000, **97**, 14046–14051.
57 P.-W. Yang, T.-L. Lin, T.-Y. Lin, C.-H. Yang, Y. Hu and U-S. Jeng, *Soft Matter*, 2013, **9**, 11542–11548.

This journal is © The Royal Society of Chemistry 2014